

# Proteomic analysis of gemcitabine-resistant pancreatic cancer cells reveals that microtubule-associated protein 2 upregulation associates with taxane treatment

Tessa Ya Sung Le Large , Btissame El Hassouni, Nicola Funel, Bart Kok, Sander R. Piersma, Thang V. Pham , Kenneth P. Olive, Geert Kazemier, Hanneke W.M. van Laarhoven, Connie R. Jimenez, Maarten F. Bijlsma and Elisa Giovannetti

## Abstract

**Background:** Chemoresistance hampers the treatment of patients suffering from pancreatic ductal adenocarcinoma (PDAC). Here we aimed to evaluate the (phospho)proteome of gemcitabine-sensitive and gemcitabine-resistant PDAC cells to identify novel therapeutic targets and predictive biomarkers.

**Methods:** The oncogenic capabilities of gemcitabine-sensitive and resistant PDAC cells were evaluated *in vitro* and *in vivo*. Cultured cells were analyzed by label-free proteomics. Differential proteins and phosphopeptides were evaluated by gene ontology and for their predictive or prognostic biomarker potential with immunohistochemistry of tissue microarrays.

**Results:** Gemcitabine-resistant cells had increased potential to induce xenograft tumours ( $p$  value < 0.001). Differential analyses showed that proteins associated with gemcitabine resistance are correlated with microtubule regulation. Indeed, gemcitabine-resistant cells displayed an increased sensitivity for paclitaxel *in vitro* ( $p$  < 0.001) and nab-paclitaxel had a strong anti-tumour efficacy *in vivo*. Microtubule-associated protein 2 (MAP2) was found to be highly upregulated ( $p$  = 0.002, fold change = 10) and phosphorylated in these resistant cells. Expression of MAP2 was correlated with a poorer overall survival in patients treated with gemcitabine in the palliative ( $p$  = 0.037) and adjuvant setting ( $p$  = 0.014).

**Conclusions:** These data show an explanation as to why the combination of gemcitabine with nab-paclitaxel is effective in PDAC patients. The identified gemcitabine-resistance marker, MAP2, emerged as a novel prognostic marker in PDAC patients treated with gemcitabine and warrants further clinical investigation.

**Keywords:** gemcitabine, nab-paclitaxel, pancreatic cancer, phosphoproteomics, proteomics, resistance

Received: 6 August 2018; revised manuscript accepted: 23 January 2019.

## Background

Pancreatic ductal adenocarcinoma (PDAC) is characterized by a high lethality, with only 7% of patients alive 5 years after diagnosis.<sup>1</sup> Most patients present with advanced disease stages, either locally advanced (stage III) or with distant

metastases (stage IV), leaving palliative chemotherapy as the only therapeutic option.<sup>2</sup> Aggressive multimodal therapy offers the best survival chances for patients diagnosed with early stage disease (stage I–IIb).<sup>3</sup> This treatment consists of a combination of resection followed by adjuvant

*Ther Adv Med Oncol*

2019, Vol. 11: 1–17

DOI: 10.1177/  
1758834019841233

© The Author(s), 2019.  
Article reuse guidelines:  
sagepub.com/journals-  
permissions

Correspondence to:  
**Elisa Giovannetti**  
Medical Oncology,  
Amsterdam UMC, Vrije  
Universiteit Amsterdam,  
Cancer Center  
Amsterdam, De Boelelaan  
1117, Amsterdam,  
Netherlands  
[e.giovannetti@vumc.nl](mailto:e.giovannetti@vumc.nl)

**Connie R. Jimenez**  
Medical Oncology,  
Amsterdam UMC, Vrije  
Universiteit Amsterdam,  
Cancer Center  
Amsterdam, Amsterdam,  
Netherlands  
[c.jimenez@vumc.nl](mailto:c.jimenez@vumc.nl)

**Maarten F. Bijlsma**  
LEXOR, Center for  
Experimental and  
Molecular Medicine,  
Amsterdam UMC,  
University of Amsterdam,  
Cancer Center  
Amsterdam, Amsterdam,  
Netherlands  
[m.f.bijlsma@gamc.uva.nl](mailto:m.f.bijlsma@gamc.uva.nl)

**Tessa Ya Sung Le Large**  
Surgery, Amsterdam  
UMC, Vrije Universiteit  
Amsterdam, Cancer  
Center Amsterdam,  
Amsterdam, Netherlands  
Medical Oncology,  
Amsterdam UMC, Vrije  
Universiteit Amsterdam,  
Cancer Center  
Amsterdam, Amsterdam,  
Netherlands  
LEXOR, Center for  
Experimental and  
Molecular Medicine,  
Amsterdam UMC,  
University of Amsterdam,  
Cancer Center  
Amsterdam, Amsterdam,  
Netherlands  
Cancer Pharmacology Lab,  
AIRC-Start-Up, University  
Hospital of Pisa, Pisa, Italy

**Btissame El Hassouni**

**Sander R. Piersma**

**Thang V. Pham**

Medical Oncology,  
Amsterdam UMC, Vrije  
Universiteit Amsterdam,  
Cancer Center  
Amsterdam, Amsterdam,  
Netherlands

**Nicola Funel**

Cancer Pharmacology Lab,  
AIRC-Start-Up, University  
Hospital of Pisa, Pisa, Italy

**Bart Kok**

**Geert Kazemier**

Surgery, Amsterdam  
UMC, Vrije Universiteit  
Amsterdam, Cancer  
Center Amsterdam,  
Amsterdam, Netherlands

**Kenneth P. Olive**

Departments of Medicine  
and Pathology and Cell  
Biology, Herbert Irving  
Comprehensive Cancer  
Center, Columbia  
University Medical Center,  
New York City, NY, USA

**Hanneke W.M. van**

**Laarhoven**

Medical Oncology,  
Amsterdam UMC,  
University of Amsterdam,  
Cancer Center  
Amsterdam, Amsterdam,  
Netherlands

chemotherapy. Currently, standard adjuvant therapy consists of six cycles of gemcitabine improving disease-free survival (DFS) from 6.7 to 13.4 months.<sup>3,4</sup>

Gemcitabine is the most commonly used cytotoxic drug backbone in Europe for the treatment of PDAC.<sup>5</sup> It is a deoxycytidine nucleoside analogue that, after intracellular transport, is phosphorylated to its activated form. The cytotoxic function is exerted *via* two mechanisms; interaction with ribonucleotide reductase results in the depletion of deoxynucleotides. In addition, gemcitabine itself is incorporated in DNA. Both functions lead to DNA synthesis arrest, followed by apoptosis and cell death.<sup>6</sup> Unfortunately, not all patients with PDAC benefit from adjuvant therapy with gemcitabine. Surgical complications and early disease progression hamper the completion of adjuvant therapy.<sup>7</sup> In addition, chemoresistance, including gemcitabine resistance, is a hallmark of PDAC biology, leading to reduced efficacy of cytotoxic agents in the adjuvant and metastatic setting. No predictive biomarkers are currently used to guide clinical decision-making for gemcitabine therapy.

The chemoresistance features of PDAC are multifactorial. These tumours are notorious for their large fibrotic tissue surrounding tumour cells in a hypovascular and hypoxic environment.<sup>8</sup> This dense tissue forms a physical barrier for drug delivery.<sup>9</sup> Moreover, cancer-associated fibroblasts reduce gemcitabine levels, further inhibiting local concentrations available to target tumour cells.<sup>10</sup> Additional paracrine and autocrine signalling axes can also impair gemcitabine efficacy.<sup>11</sup>

Most importantly, PDAC cells themselves harbour several intrinsic resistance mechanisms that overcome cytotoxic effects. For example, epithelial-to-mesenchymal transition (EMT) and the existence of cancer stem cell (CSC) subclones can contribute to intrinsic resistance.<sup>12-14</sup>

Previously, Quint and colleagues<sup>13</sup> established a resistant subclone of a pancreatic cancer cell line after short-term treatment with a high dose of gemcitabine in order to study the potential mechanisms of gemcitabine resistance. These gemcitabine-resistant cells exhibited increased mRNA of EMT and CSC markers, as well as a significantly enhanced capability to migrate. We hypothesized that by analyzing this model, novel prognostic/predictive protein markers could be

identified and that their expression and phospho-protein state could guide innovative therapeutic approaches. To this aim, we investigated protein expression in-depth and evaluated pathway activation of gemcitabine-resistant cells *via* an unbiased proteomic approach. We found that gemcitabine-resistant PDAC cells are sensitive to taxane-based treatment *in vitro* and *in vivo*. Furthermore, we uncovered microtubule-associated protein 2 (MAP2) as a potential biomarker for gemcitabine resistance in two cohorts of PDAC patients.

## Methods

### *Cell culture and drugs*

In this study, a gemcitabine-sensitive cell line, PANC1, and a gemcitabine-resistant PANC1 cell line, PANC1R, were kindly supplied by the Institute for Surgical Research, Philipps-University of Marburg, Marburg, Germany.<sup>13</sup> Cells were cultured in Roswell Park Memorial Institute (RPMI) medium (Lonza, Switzerland) supplemented with 10% heat-inactivated foetal calf serum (Biowest, Nuaille, France) and 1% penicillin and streptomycin (Lonza, Switzerland). Cells were maintained at low passage and tested negatively for mycoplasma contamination. Hs766t cells and Capan-2 (ATCC, Manassas, USA) were cultured in supplemented Dulbecco's Modified Eagle Medium (Lonza) and several primary cell lines (PDAC1-4)<sup>15</sup> and Capan-1 (ATCC) were grown at low density in supplemented RPMI medium. Paclitaxel (Bristol-Meyers Squibb, New York, USA) and docetaxel (Sigma-Aldrich, St. Louis, USA) were dissolved in 50% ethanol and sterile H<sub>2</sub>O. Gemcitabine was kindly provided by Eli Lilly Corporation (Indianapolis, USA) and dissolved in sterile water. Nab-paclitaxel was kindly supplied by the Pharmacy of New York Presbyterian Hospital (New York, NY, USA) and was dissolved in NaCl.

### *Cell lysis and protein digestion*

Cell line lysates were prepared as described before in 9 M urea buffer containing 4-(2-hydroxyethyl)-1-piperazineethanesulfonic acid (HEPES) and phosphatase inhibitors.<sup>16</sup> Biological duplicates of different passages were prepared. Lysates were sonicated on ice and protein concentration was measured using the Bicinchoninic Acid (BCA) method (ThermoPierce, Waltham, USA). For protein expression analysis, protein digestion and

extraction was performed with our whole-in-gel protocol described previously.<sup>17</sup> In short, 50  $\mu\text{g}$  of protein was mixed with NUpage lithium dodecyl sulfate (LDS) sample buffer (Invitrogen, Carlsbad, USA) containing dithiothreitol (DTT; Sigma-Aldrich, St. Louis, USA) and loaded on a NUpage 4–12% gradient gel (Invitrogen). After electrophoresis, gels were fixed and stained with Coomassie Brilliant Blue solution. After reduction and alkylation, proteins were digested overnight with trypsin (Promega, Madison, USA) and extracted from the gel for further analysis.

### *Phosphopeptide enrichment*

For phosphoprotein analysis, 500  $\mu\text{g}$  of lysates were digested in solution after reduction and alkylation. Digestion was stopped by acidification and phosphopeptides were enriched according to our laboratory's protocol.<sup>16</sup> Briefly, peptides were desalted with C18 cartridges (Waters, Milford, USA). Global phosphopeptide enrichment was performed using titanium dioxide beads (10  $\mu\text{m}$ , GL Sciences, Tokyo, Japan) using 300 mM lactic acid and 80% acetonitrile (ACN). Phosphopeptides were eluted by 0.5% and 5% piperidine. After enrichment, phosphopeptides were desalted in 20  $\mu\text{l}$  StageTips using 0.1% trifluoroacetic acid (TFA) and were eluted with 80% ACN/0.1% TFA into glass-lined autosampler vials. Eluates were dried in a speed-vac and resolved in 20  $\mu\text{l}$  loading solvent (4% ACN in 0.5% TFA) and stored at 4°C until liquid chromatography-mass spectroscopy (LC-MS)/MS measurement on the same day.

### *Nano-LC-MS/MS and protein identification*

Peptides were separated by an Ultimate 3000 nanoLC-MS/MS system (Dionex LC-Packings, Amsterdam, the Netherlands) equipped with a 40 cm  $\times$  75  $\mu\text{m}$  ID fused silica column custom packed with 1.9  $\mu\text{m}$  120 Å ReproSil Pur C18 aqua (Dr Maisch GMBH, Beim Brückle, Germany). After injection, peptides were trapped at 6  $\mu\text{l}/\text{min}$  on a 10 mm  $\times$  100  $\mu\text{m}$  ID trap column packed with 5  $\mu\text{m}$  120 Å ReproSil Pur C18 aqua at 2% buffer B [buffer A: 0.5% acetic acid (Fischer Scientific, Hampton, USA), buffer B: 80% ACN, 0.5% acetic acid] and separated at 300 nl/min in a 10–40% buffer B gradient in 90 min (120 min inject-to-inject) at 35°C. Eluting peptides were ionized at a potential of +2 kV into a Q Exactive mass spectrometer (Thermo Fisher, Erlangen, Germany). Intact masses were measured at

resolution 70,000 (at  $m/z$  200) in the orbitrap using an Automatic Gain Control (AGC) target value of  $3 \times 10^6$  charges. The top 10 peptide signals (charge states 2+ and higher) were submitted to tandem mass spectrometry (MS/MS) in the Higher-energy collisional dissociation (HCD) (higher-energy collision) cell (1.6 amu isolation width, 25% normalized collision energy). MS/MS spectra were acquired at resolution 17,500 (at  $m/z$  200) in the orbitrap using an AGC target value of  $2 \times 10^5$  charges and an under-fill ratio of 0.1%. Dynamic exclusion was applied with a repeat count of 1 and an exclusion time of 30 s.

### **Protein identification**

MS/MS spectra were searched against the uniprot human reference proteome 2014\_01\_NO\_fragments FASTA file (61,552 entries) using MaxQuant 1.5.2.8<sup>18</sup> (protein expression) and the 2015\_08\_NO\_fragments FASTA file (62,447 entries; phosphoproteomics). Enzyme specificity was set to trypsin and up to two missed cleavages were allowed. Cysteine carboxyamidomethylation (Cys, +57.021464 Da) was treated as fixed modification and serine, threonine and tyrosine phosphorylation (+79.966330 Da), methionine oxidation (Met, +15.994915 Da) and N-terminal acetylation (N-terminal, +42.010565 Da) as variable modifications. Peptide precursor ions were searched with a maximum mass deviation of 4.5 ppm and fragment ions with a maximum mass deviation of 20 ppm. Peptide, protein and site identifications were filtered at an false discovery rate (FDR) of 1% using the decoy database strategy. The minimal peptide length was 7 amino-acids and the minimum Andromeda score for modified peptides was 40 and the corresponding minimum delta score was 6. Proteins that could not be differentiated based on MS/MS spectra alone were grouped to protein groups (default MaxQuant settings). Phosphopeptide identifications were propagated across samples using the match between runs option checked. Protein expression searches were performed with the label-free quantification option selected.

### **Label-free phosphopeptide quantification**

Phosphopeptides were quantified by their extracted ion intensities ('Intensity' in MaxQuant). For each sample, the phosphopeptide intensities were normalized on the median intensity of all identified phosphopeptides of the dataset ('normalized intensity').

### Label-free protein quantification

Proteins were quantified by spectral counting, that is, the number of identified MS/MS spectra for a given protein. Raw counts were normalized on the sum of spectral counts for all identified proteins in a particular sample, relative to the average sample sum determined with all samples. Identified proteins and phosphopeptides are listed in Supplemental Table 1(a and b), respectively. Supplemental Table 1(c) contains identified phosphosites.

The MS proteomics data have been deposited to the ProteomeXchange Consortium *via* the PRIDE<sup>19</sup> partner repository with the dataset identifier PXD010112.

### Drug inhibitory assays

For the drug inhibitory assays, PANC1 and PANC1R cells were seeded in triplicate onto 96-wells plates with a density of 3000 cells per well. Hs766t, Capan2, Capan1 and PDAC1-4 were seeded with a density of 3000–5000 cells per well. Cells were attached overnight and cytotoxic drugs (paclitaxel, docetaxel, gemcitabine) were added in different concentration ranges. Drugs were incubated for 72h, after which proteins of viable cells were precipitated and subsequently stained with sulforhodamine B (SRB) and measured for absorbance at 492 nm in the Synergy microplate reader (Biotek Cytation3 Cell Imaging Multi-Mode Reader, Winooski, USA). The inhibitory concentration of 50% of the cells (IC<sub>50</sub>) was determined by nonlinear least squares curve fitting with Graphpad Prism (version 7.0, Intuitive Software for Science, San Diego, USA). For combination treatment, a fixed concentration of paclitaxel combined with gemcitabine was evaluated against a dose-response curve of gemcitabine alone.

### Immunofluorescence

Cells were plated in Chamber-Slides System (Lab-Tek, Thermo Fisher Scientific, Waltham, USA) with a density of 10<sup>4</sup> per well and attached overnight. Cells were treated with gemcitabine (1 μM) or vehicle for 24 hours. Subsequently, cells were fixed with 4% paraformaldehyde and stained with a specific monoclonal rabbit anti-human MAP2 antibody (1:200, #MA5-12823), followed by Alexa Fluor 594 goat anti-rabbit (Product#A-11032) and anti-mouse (Cat#A-11032). Nuclear DNA was stained with 4',6-diamidino-2-phenylindole (DAPI). Digital images were

captured with a Zeiss Laser Scanning Microscope and processed with Axiovision 4.1 software (Zeiss Microimaging, Thornwood, USA).

### Western blot analysis

In brief, 20 μg of total protein was loaded on 10% sodium dodecyl sulphate/polyacrylamide gels after denaturation. After electrophoresis, proteins were transferred onto nitrocellulose membranes (Millipore, Temecula, USA) overnight. Membranes were blocked in 5% blotting-grade blocker nonfat dry milk (Biorad, Hercules, USA) in phosphate buffered saline (PBS) and 0.1% Tween20 (PBST). Primary antibodies were incubated in 5% bovine serum albumin (Sigma-Aldrich) in PBST at room temperature and membranes were subsequently washed and incubated with secondary antibodies in 5% blocking buffer. Proteins were detected with SuperSignal West Pico Chemoluminescent substrate (Thermo Scientific, Waltham, USA) and visualized by an Uvitec Imaging station (Clever Scientific, Rugby, UK). Antibodies used for western blot analysis were anti-MAP2 (1:200, Invitrogen), anti-ankyrin-3 (ANK3; 1: 1000, HPA0556439, Human Protein Atlas), anti-nestin (NES; 1:200, HPA007007, Human Protein Atlas), anti-beta-actin (1:1000, CA # 4967S, Cell Signaling), anti-mouse-horseradish peroxidase (HRP; 1:2000, CA # 7076S, Cell Signaling), anti-rabbit-HRP (1:2000, CA# 7074S, Cell Signaling).

### Quantitative real-time polymerase chain reaction

Quantitative real-time polymerase chain reaction (RT-qPCR) was performed according to a previous protocol.<sup>20</sup> In short, cells were harvested in Trizol Reagent (ThermoFisher, Waltham, USA) and RNA was isolated according to the manufacturer's protocol. Complimentary DNA (cDNA) was created with a DyNAmo cDNA Synthesis Kit (ThermoFisher). RT-qPCR was performed on the CFX Manager CFX96 (Biorad) with MAP2 and ACTB primers (Taqman, code 4453320 and 4326315E respectively). The ΔΔCT method was used to evaluate MAP2 expression levels compared with PANC1, and to evaluate MAP2 expression upon gemcitabine treatment.

### Fluorescence-activated cell sorting analysis

For microtubule stabilization analysis, fluorescence-activated cell sorting analysis was

performed as described previously.<sup>21</sup> In short, cells were seeded and treated with either vehicle or paclitaxel (200 ng/ml). After incubation of 2 h, cells were harvested, fixed and microtubules stabilized. Staining was performed with anti-tubulin-Fitc conjugated antibody (1:50, CA #8058 Cell Signaling). Cells were analyzed by flow cytometry on a FACSCalibur (Becton Dickinson, Franklin Lakes, USA) in triplicate.

#### *In vivo tumorigenesis and drug evaluation*

Mouse experiments were performed in accordance with the National Institutes of Health Guidelines for animal research and procedures were approved by the Institutional Animal Care and Use Committee of the Columbia University (IACUC; number AC-AAAQ1415). A total of 36 mice were utilized in this study. To establish xenograft tumours, 50 µl containing  $3 \times 10^6$  cells, suspended in 50% sterile Matrigel and PBS, were injected into the flanks of 6–8-week-old athymic nude mice (Taconic Labs & the Jackson Laboratory, Rensselaer, New York, USA). A total of 18 mice in each arm were inoculated with either PANC1 or PANC1R cells. Growth of tumours was evaluated weekly by ultrasound (Verasonics, Kirkland, USA) while mice were anaesthetized with 1–2% isoflurane (Halocarbon, Peachtree Corners, USA) in oxygen. A 3D positioner (Velmex Inc., Bloomfield, USA) was used to mechanically ultrasound the full tumour with 1-mm horizontal step-wise imaging. Volumetric reconstructions were performed to evaluate tumour volume and growth. Mice were enrolled once their tumour size was at least 100 mm<sup>3</sup>. They were treated intravenously with either vehicle (NaCl) as control or nab-paclitaxel (60 mg/kg). They received three doses of treatment over a period of 8 days. During treatment and tumour progression, tumour volume was evaluated twice a week. If no tumour residue or progression was observed after treatment, mice were censored at day 120. End points were tumour volume larger than 1000 mm<sup>3</sup>, weight loss over 20% after start of treatment or clinical signs of suffering. Mice were excluded from survival analysis if they suffered from extreme side effects from therapy within the first 8 days ( $n = 2$ ). Tumour tissues were stored in formalin-fixed paraffin embedded (FFPE) blocks.

#### *Tissue microarrays*

To evaluate novel proteins as prognostic biomarker in relation with gemcitabine response, two patient

cohorts were evaluated. The first cohort consisted of metastatic patients (stage IV,  $n = 36$ ) treated with gemcitabine in the palliative setting. The second validation cohort consisted of early stage patients (stage I–IIb,  $n = 86$ ) treated with gemcitabine in the adjuvant setting. Representative cores of individual primary PDAC FFPE tissues prior to treatment were selected and combined in tissue microarrays (TMAs). Immunohistochemistry (IHC) staining of MAP2 was performed according to manufacturer's protocol. As a positive control, human brain cortex FFPE material was used. As negative control, slides stained with no primary antibody were used. Visualization was obtained with BenchMark Special Stain Automation system (Ventana Medical Systems, Export, USA). Staining was evaluated by a molecular pathologist, assessing the amount of tumour and tissue loss, background, and overall interpretability. Immunostaining intensity was classified into two grades: 0 (absent) and 1 (present). All patients provided written informed consent for the storage, analysis of their tumour material and survival data. This study was approved by the Local Ethics Committee of the University of Pisa (Ethics approval no 3909, on 3 July 2013) and patients signed an informed consent for the use of tissue samples.

#### *Statistics*

Data were analyzed with Graphpad Prism Software, version 7 (Intuitive Software for Science, San Diego, USA), R Project (version 3.3.4) and SPSS, version 21 (IBM, Chicago, USA). Differential expression of proteomic data was analyzed with the beta-binomial test.<sup>22</sup> Fold changes (FCs) were expressed per group comparison. Heatmap visualization and hierarchical clustering was done with R package gplots (Euclidean distance function, with default complete linkage). Gene ontology mining was performed with Cytoscape, version 3.5.0, in addition with the ClueGO, version 2.5.0.<sup>23</sup> *In vitro* experiments were performed with a minimum of three biological replicates. Curves were compared by nonlinear regression analysis and the F test. Group comparisons were evaluated with the unpaired nonparametric Mann–Whitney *U* test or unpaired Student's *t* test. Fishers exact test was used for categorical analysis. Correlation with clinicopathological characteristics, including progression-free survival (PFS) or DFS and overall survival (OS), was tested with Kaplan–Meier curves and the log-rank test. Univariate analysis was performed and factors with a *p* value below

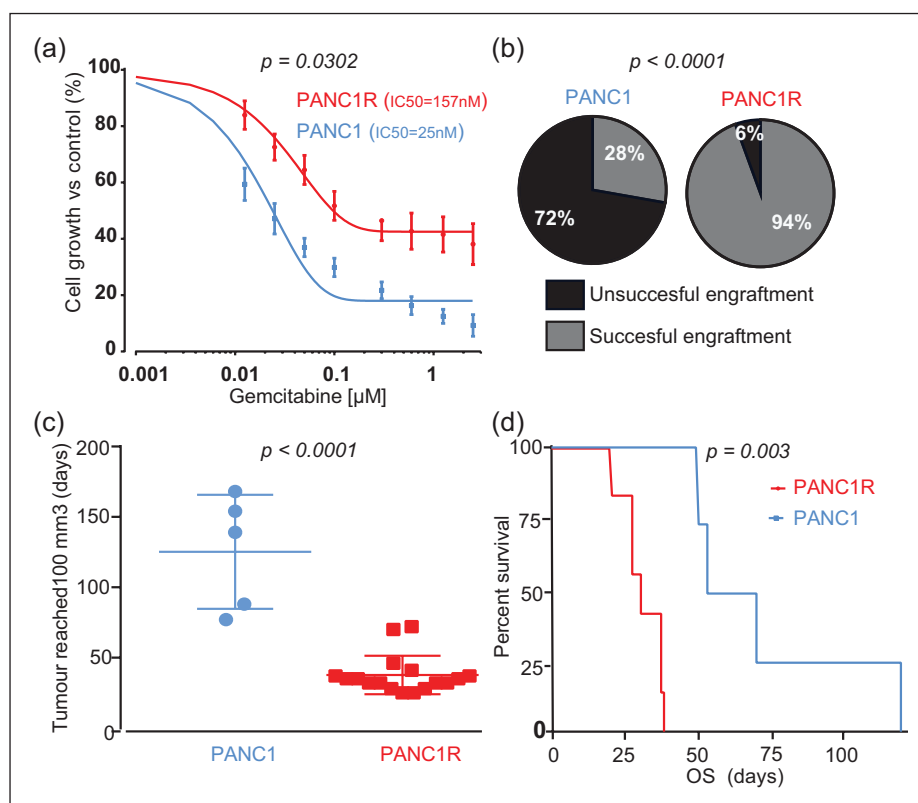


**Figure 1.** Characterization of sensitive PANC1 and resistant PANC1R cells *in vitro* and *in vivo*. (a) Dose-response curves of PANC1 (blue) and PANC1R (red) cells display a reduced sensitivity to gemcitabine. Points and bars, mean values and SEM obtained from 10 independent experiments. (b) PANC1R cells induce significantly more tumours by subcutaneous engraftment ( $n = 36$ , 18 mice per arm) than PANC1 cells. (c) Tumours originating from PANC1R developed an evident tumour nodule faster. (d) Tumours of PANC1R origin resulted in poorer OS (Day 0 was set for each mouse individually based on reaching evident tumour volume of 100 mm<sup>3</sup>). Of note, groups in survival analysis were unequal due to poor engraftment success of PANC1 cells ( $n = 4$  versus  $n = 7$ ). OS, overall survival; PANC1, gemcitabine-sensitive cell line; PANC1R, gemcitabine-resistant PANC1 cell line.

0.1 were evaluated in the multivariate analysis according to the Wald model. Statistical significance was set at  $p$  values below 0.05.

## Results

### *In vitro and in vivo characterization of gemcitabine-resistant PDAC cells*

Gemcitabine-resistant PDAC cells survived treatment with higher doses of gemcitabine [Figure 1(a), F test on log-IC<sub>50</sub>,  $p = 0.032$ ] compared with sensitive PANC1 cells. To evaluate tumorigenic capabilities, we performed an *in vivo* experiment. Only 28% of nude mice harboured a xenograft tumour within 90 days after subcutaneous injection with PANC1 cells, compared with an implantation rate of 95% upon injection with the gemcitabine-resistant PANC1R cells [Figure 1(b), Fisher's exact test  $p < 0.0001$ ]. Upon

successful tumour engraftment, PANC1R tumours developed an evident tumour nodule, defined by a volume of 100 mm<sup>3</sup>, significantly faster than PANC1 cells [Figure 1(c), median 35 versus 139 days, Mann-Whitney  $U$  test,  $p < 0.0001$ ]. Moreover, PANC1R mice reached their endpoint faster [Figure 1(d), median OS 30 versus 61.5 days, log-rank test  $p = 0.003$ ]. These results highlight the enhanced take rate and growth rate of these gemcitabine-resistant PDAC cells *in vivo*.

### Differential protein expression and pathway analysis

Protein expression and protein phosphorylation are tightly regulated mechanisms to induce protein activity and regulate biological functions.<sup>24</sup> To explore the underlying tumorigenic capability, and understand the biology of gemcitabine-resistant cells,

we performed an unbiased protein expression and protein phosphorylation analysis by MS. We obtained a dataset of 6074 proteins [Supplemental Table 1(a)] and 10,623 phosphopeptides [Supplemental Table 1(b)], mapping to 2626 phosphoproteins with 262 proteins and 143 phosphopeptides differentially regulated in gemcitabine-resistant PANC1R cells compared with sensitive PANC1 cells [Supplemental Table 1(e and f)]. Biological replicates of both cell lines cluster together, indicating differential biology (Supplemental Figure 1). Since PANC1R cells were proven resistant to gemcitabine, gemcitabine pathway elements and known resistance mechanisms (e.g. membrane transporters, CSC markers) were evaluated (Supplemental Table 2). The gemcitabine transporter SLC29A1 (ENT) was decreased (FC = -1.5), while the dephosphorylating enzyme NT5C was increased (FC = 2.3) in PANC1R, although both not significantly. These two shifts in gemcitabine pathway modulators could partly explain the gemcitabine-resistant phenotype.<sup>25,26</sup> Anion-exchange transporters SLC5A3 and SLC4A2 were significantly upregulated, while SLC25A5 and SLC7A6 were significantly downregulated. However, these transporters have no known functions in resistance against anticancer drugs. Overall expression of CSC markers was inconclusive between the two cell lines indicating no clear relation of CSC markers with resistance in our cells. To further understand the biological features that underlie the differential sensitivity to gemcitabine between PANC1 and PANC1R, gene ontology mining was performed. Upregulated proteins of PANC1R cells were enriched in biological processes of regulation of (endo)membrane and cell projection organization. Moreover, these cells express proteins associated with vesicle localization, a possible method for drug resistance *via* drug efflux mechanisms *via* vesicles<sup>27</sup> [Supplemental Figure 2(a and b)]. Observed downregulated processes involved metabolic and differentiation processes. Downregulated phosphorylation events were correlated with intrinsic apoptotic signaling pathways to DNA damage. This potentially indicates another adaptation to gemcitabine response in our resistant cells. Interestingly, upregulated phosphoproteins were associated with microtubule regulation [Supplemental Figure 3(a and b)], which could highlight a therapeutic window for microtubule inhibitors.

### Exploration of microtubule inhibitors as a therapeutic option

Given the established clinical effectiveness of combining gemcitabine with the microtubule

stabilizing agent nab-paclitaxel<sup>28</sup> and our finding of upregulation of microtubule-associated processes in a gemcitabine-resistant cell line, we next evaluated the effect of microtubule inhibitors on our *in vitro* model. The two microtubule stabilizing agents, paclitaxel and docetaxel, were both effective against gemcitabine-sensitive and resistant cells [Supplemental Figure 4(a)]. Interestingly, cell viability was more affected in gemcitabine-resistant cells than in the gemcitabine-sensitive cells at low paclitaxel doses [Figure 2(a), unpaired Student's *t* test  $p = 0.0082$  and  $0.0335$ , respectively]. This difference diminished when exposing cells to higher concentrations of paclitaxel (>5 nM,  $p = \text{ns}$ ). Conversely, docetaxel had an equal impact on viability of PANC1 and PANC1R cells [Supplemental Figure 4(a)]. These results are important since they underline that chemoresistant mechanisms can be drug-specific, highlighting opportunities for other therapeutic targets when the disease progresses during gemcitabine treatment.

To understand the mechanism of enhanced paclitaxel toxicity in PANC1R, we quantified microtubule polymerization, the target of paclitaxel. Upon treatment, PANC1R cells showed significant increase in microtubule stabilization [Supplemental Figure 4(b)]. This suggests that the increased sensitivity to paclitaxel of resistant cells can be attributed to the increased microtubule stabilization effect of taxanes in these cells. Moreover, combination treatment with gemcitabine and a fixed dose of paclitaxel resulted in an increased inhibition of proliferation of resistant cells compared with monotherapy with gemcitabine [Supplemental Figure 4(c)]. These findings provide functional proof for combination treatment to target gemcitabine-resistant cells in PDAC tumours.

To further validate our results, mice harbouring PANC1R tumours were treated with three doses of nab-paclitaxel ( $n = 7$ ), a paclitaxel-derivative bound to albumin, which is currently registered in the clinic for multiple solid tumour types including metastatic PDAC<sup>28</sup> or were treated with vehicle ( $n = 7$ ). Nab-paclitaxel-treated mice showed significantly improved survival [Figure 2(b)] and effective tumour growth inhibition [Figure 2(c), Supplemental Figure 5]. In five out of seven mice, treatment resulted in complete tumour regression. These results suggest that gemcitabine-resistant cells can be effectively targeted by (nab-)paclitaxel and suggests that the

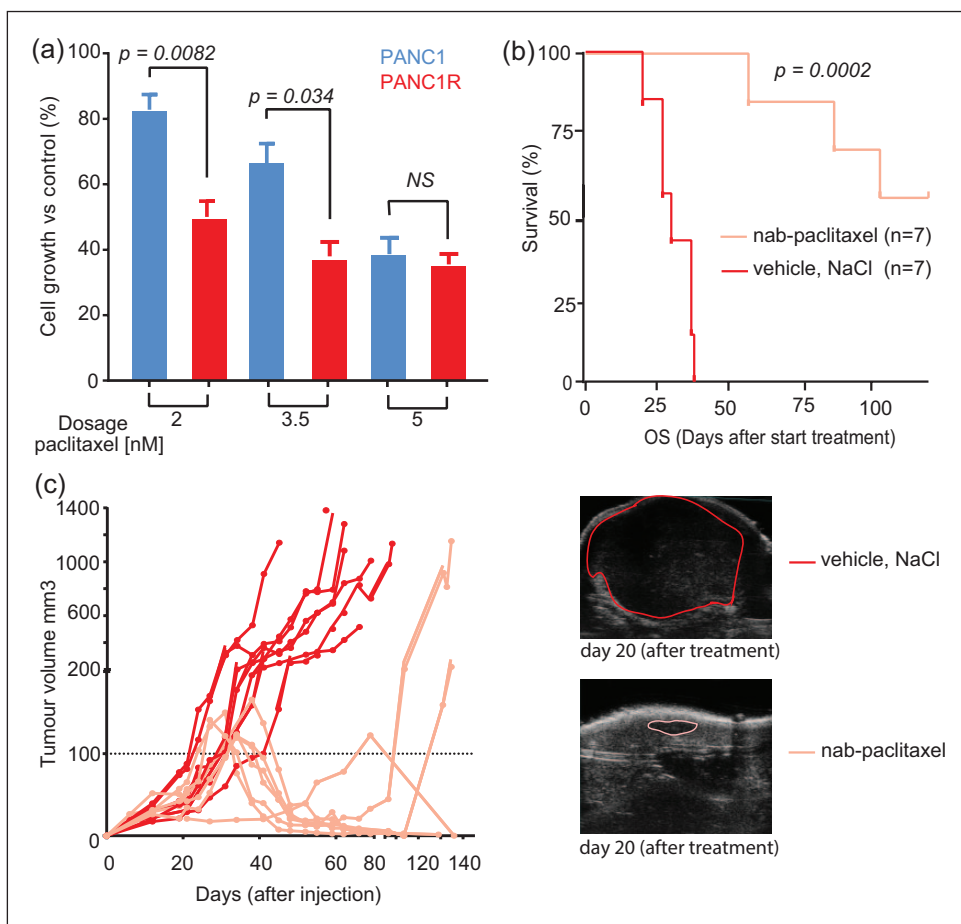


**Figure 2.** Cytotoxic effects of (nab-)paclitaxel on resistant PANC1R cells *in vitro* and *in vivo*.

(a) Resistant cells were significantly more sensitive to paclitaxel treatment *in vitro*. Columns and bars, mean and SEM values obtained from three independent experiments. (b) Treatment with nab-paclitaxel ( $n = 9$ , three doses of 60 mg/kg) versus vehicle ( $n = 7$ , NaCl) resulted in improved survival *in vivo*. The two mice treated with nab-paclitaxel were excluded from the analysis in the treatment arm due to side effects from the treatment forcing a humane endpoint before the end of treatment. (c) Tumour growth was evaluated by ultrasound (example on the right panel), showing continuous growth of the tumour in vehicle-treated mice, whereas mice treated with nab-paclitaxel had obvious tumour regression. Dashed black line indicates the 100 mm<sup>3</sup> volume of the tumour upon treatment was started. A total of five mice had no measurable residual tumour after treatment and no outgrowth during follow up.

PANC1R, gemcitabine-resistant PANC1 cell line; SEM, standard error of the mean

efficacy of gemcitabine with the addition of nab-paclitaxel in patients might not only rely on drug synergism, but also on targeting of resistant subclones.

### Validation of MAP2 as a predictive marker of gemcitabine sensitivity

In the proteomic screen, several upregulated proteins were identified in the gemcitabine-resistant cells (Table 1) and we reasoned that these proteins could be predictive for gemcitabine resistance in patients. A total of three proteins were selected, based on FCs and significant upregulation in resistant cells; MAP2, ANK3 and NES.

Western blot analysis validated our proteomic analysis for MAP2 and ANK3 as upregulated proteins in our cell-line model [Figure 3(a)]. Unfortunately, low levels of NES precluded quantitative evaluation and this candidate was omitted from further analysis.

To validate the clinically applicable value of our proteome screen, MAP2 and ANK3 protein expression were evaluated by IHC on two independent PDAC cohorts. The first cohort consisted of metastatic patients who received gemcitabine monotherapy in the palliative setting. The second cohort encompassed stage IIB patients who received gemcitabine as adjuvant



**Table 1.** Top 10 upregulated proteins and phosphoproteins in gemcitabine-resistant PANC1 cells *versus* sensitive cells. Proteins or peptides were filtered based on a FC increase of minimally 2.5-fold and ordered on *p* value. NA indicates that the protein was not identified in one of the groups, thus a FC could not be calculated.

Top 10 upregulated proteins				Top 10 upregulated phosphopeptides				
gene name	protein name	<i>p</i> value	FC	gene name	protein name	p-peptide sequence	<i>p</i> value	FC
MAP2	Microtubule-associated protein 2	0.0002	10.18	MAP2	Microtubule-associated protein 2	VDHGAEIITQSPGRSSVASPR	0.0054	18.04
ANK3	Ankyrin-3	0.0005	22.81	KIF1A	Kinesin-like protein KIF1A	DVLSPLRPSR	0.0092	2.61
NES	Nestin	0.0006	6.33	TMCC3;TMCC2	Transmembrane and coiled-coil domains protein 3	NKFGSADNIAHLK	0.0131	6.09
CAT	Catalase	0.0013	2.52	TACC2	Transforming acidic coiled-coil-containing protein 2	MSESPTPCSGSSFEETEALVNTAAK	0.0139	7.11
KIF1A	Kinesin-like protein KIF1A	0.0018	4.49	ARHGEF16	Rho guanine nucleotide exchange factor 16	GLGKPGGGDDAIQLSPK	0.0209	3.79
STAT6	Signal transducer and activator of transcription 6	0.0019	NA	ABCC1	Multidrug resistance-associated protein 1	QLSSSSSYSGDISR	0.0258	4.61
HTT	Huntingtin	0.0019	2.58	MAP2	Microtubule-associated protein 2	RKSVPSETWEDSR	0.0350	10.10
GSTM2	Glutathione S-transferase Mu 2	0.0020	NA	PPFIBP1	Liprin-beta-1	NSPFQIPPPSPDSK	0.0362	2.91
CACHD1	VWFA and cache domain-containing protein 1	0.0028	NA	LSR	Lipolysis-stimulated lipoprotein receptor	SVDALDDLTPPSTAESGSRPTSNGGR	0.0396	3.42
MAPRE2	Isoform 4 of microtubule-associated protein RP/EB family member 2	0.0028	NA	ZFYVE19	Abscission/NoCut checkpoint regulator	LPDSDDEDEETAQR	0.0403	3.41

FC, fold change; PANC1, gemcitabine-sensitive cell line.

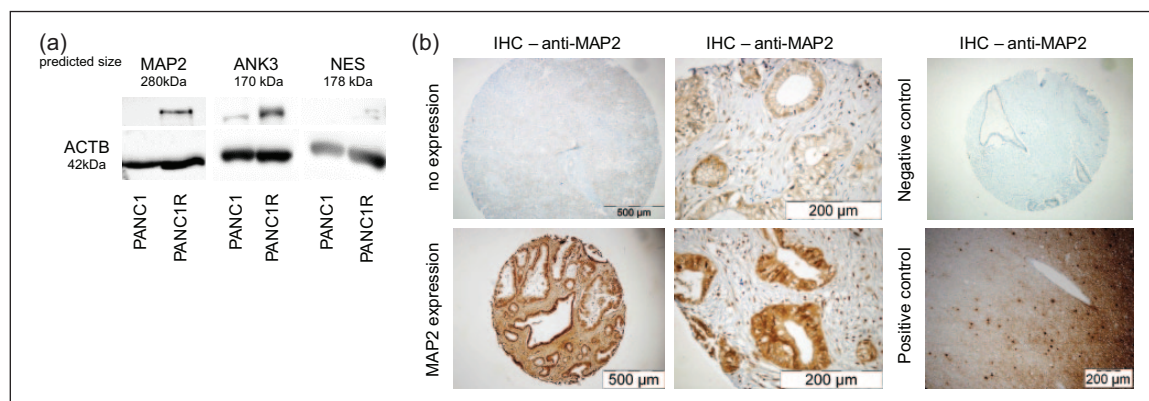


**Figure 3.** Identification of predictive markers of gemcitabine resistance.

(a) Western blot analysis of possible predictive biomarkers shows evident overexpression of MAP2 and ANK3 in PANC1R cells compared with the sensitive PANC1, in concordance with the MS/MS results. NES was expressed too low to be quantified properly. (b) Evaluation of MAP2 expression in TMAs. Representative images of TMA cores (4×) and images at higher magnification (40×) of a positive and negative staining of MAP2 in the glandular tumour islands. As a negative control (4×), slides without primary antibody was used. As a positive control (10×), human brain cortex was used. MAP2, microtubule-associated protein 2; MS/MS, tandem mass spectrometry; NES, Nestin; PANC1, gemcitabine-sensitive cell line; PANC1R, gemcitabine-resistant PANC1 cell line; TMA, tissue microarray.

therapy after resection of the primary tumour (clinicopathological characteristics of both cohorts are shown in Table 2). Of note, sex was significantly correlated with OS in these cohorts. ANK3 was expressed at equal levels in all tumours and scoring on high *versus* low expression did not predict gemcitabine resistance. MAP2 had a variable expression pattern between patients [Figure 3(b)]. Positive staining for MAP2 correlated significantly with shorter OS in metastatic patients [Figure 4(a), median OS 11 *versus* 7.5 months, log-rank test  $p = 0.037$ ], in line with our cell line and xenograft model [Figure 5(a and b)]. A trend towards worse PFS in this cohort was also seen (log-rank test  $p = 0.1$ ). Moreover, MAP2 expression in surgical specimens of patients subsequently treated with adjuvant therapy was correlated to decreased OS [Figure 4(b), median OS 21.7 *versus* 15.1 months, log-rank test  $p = 0.014$ ] and DFS [log-rank test  $p = 0.010$ , Figure 4(c)]. High expression of MAP2 was not correlated with other clinicopathological features. In the multivariate analysis, MAP2 and sex were prognostic factors for OS. MAP2 expression emerged also as an independent prognostic factor for a worse DFS (Table 2). To further explore the possible predictive value of MAP2 and gemcitabine resistance, we evaluated primary cell lines and ATCC lines for MAP2 expression. MAP2 was identified as upregulated on mRNA level in our model by RNAseq<sup>29</sup> [Supplemental Figure 6(a)]. Interestingly, high expression of MAP2 was not a common feature in PDAC cell lines, which

is in concordance with our clinical data, which showed 19% MAP2 positivity in both cohorts (Table 2). Cell line Hs766t showed high baseline expression of MAP2 [Supplemental Figure 6(b)]. High or intermediate expression of MAP2 was associated with reduced efficacy of gemcitabine [Supplemental Figure 6(c)]. Importantly, all cells were sensitive to paclitaxel treatment (IC<sub>50</sub> range from 1.4 to 14.6 nM), irrespective of their gemcitabine sensitivity levels. Of note, Capan1, a cell line with low MAP2 mRNA, showed an increase of MAP2 upon treatment of gemcitabine, further supporting the potential role of this protein in inducing a rapid mechanism of acquired resistance [Supplemental Figure 6(d)], but further studies are needed in order to develop additional appropriate models of resistance.

## Discussion

We used comprehensive proteomic and phosphoproteomic strategies to understand the gemcitabine-resistant mechanism in our PDAC model and to evaluate treatment options. We identified MAP2 as an upregulated protein in gemcitabine-resistant cells. Gemcitabine-resistant cells expressing MAP2 had an increased sensitivity to (nab-)paclitaxel treatment *in vitro*, induced significant tumour reduction *in vivo*, and showed a benefit of combination therapy with gemcitabine. Moreover, MAP2-positive staining was validated as a prognostic biomarker in two patient cohorts treated with gemcitabine monotherapy, either in

**Table 2.** Clinicopathological characteristics of two TMA cohorts.

Clinicopathological characteristics		Adjuvant cohort								
Metastatic cohort		n (%)	OS months (95% CI)	p value	n (%)	OS months (95% CI)	p value	n (%)	DFS months (95% CI)	p value
Univariate analysis										
No. patients		36 (100)	8.54 (5.60–11.43)		86 (100)	21.02 (14.21–19.73)		86 (100)	17.58 (15.62–19.55)	
<b>Age, year (at time of diagnosis)</b>				0.103			0.225			0.215
>65		21 (58)	9.09 (7.251–10.928)		29 (34)	18.14 (15.6–21.79)		29 (34)	16.05 (13.13–18.96)	
<65		15 (42)	12.14 (8.73–15.55)		57 (66)	21.46 (17.96–24.95)		57 (66)	18.37 (15.80–20.93)	
<b>Sex</b>				0.259			0.012			0.291
Female		11 (31)	12.37 (9.65–15.10)		38 (44)	24.13 (19.85–28.41)		38 (44)	19.08 (16.14–22.02)	
Male		25 (69)	9.47 (7.20–11.75)		48 (56)	17.50 (14.56–20.44)		48 (56)	16.40 (13.77–19.03)	
<b>Disease stage no. (%)</b>										
Stage I		0			0			0		
Stage IIA		0			0			0		
Stage IIB		0			86 (100)			86 (100)		
Stage III		0			0			0		
Stage IV		36 (100)			0			0		
<b>Tumour grade</b>				0.252			0.118			0.068
Grade 1–2		15 (42)	11.90 (8.65–15.16)		43 (50)	22.40 (18.16–26.65)		43 (50)	19.71 (16.63–22.80)	
Grade 3		21 (58)	9.26 (7.24–11.28)		43 (50)	18.46 (15.56–21.35)		43 (50)	15.45 (13.15–17.76)	
<b>MAP2 expression</b>				0.037			0.014			0.011
Yes		7 (19)	7.48 (5.53–9.44)		16 (19)	15.06 (12.03–18.09)		16 (19)	13.28 (10.46–16.10)	
No		29 (81)	11.06 (8.91–13.2)		70 (81)	21.66 (18.62–24.70)		70 (81)	18.57 (16.29–20.84)	
<b>Multivariate analysis</b>										
Sex (female versus male)					1	0.542 (0.347–0.845)				0.007
Grading (3 versus 1–2)					1	1.446 (0.934–2.238)				0.098
MAP2 expression (yes versus no)					1	2.225 (1.249–3.962)				0.007
<b>Multivariate analysis</b>										
Risk of death, HR (95% CI)										
Risk of relapse, HR (95% CI)										

CI, confidence interval; df, degrees of freedom; DFS, disease-free survival; HR, hazard ratio; OS, overall survival; MAP2, microtubule-associated protein 2; PANC1, gemcitabine-sensitive cell line; TMA, tissue microarray.

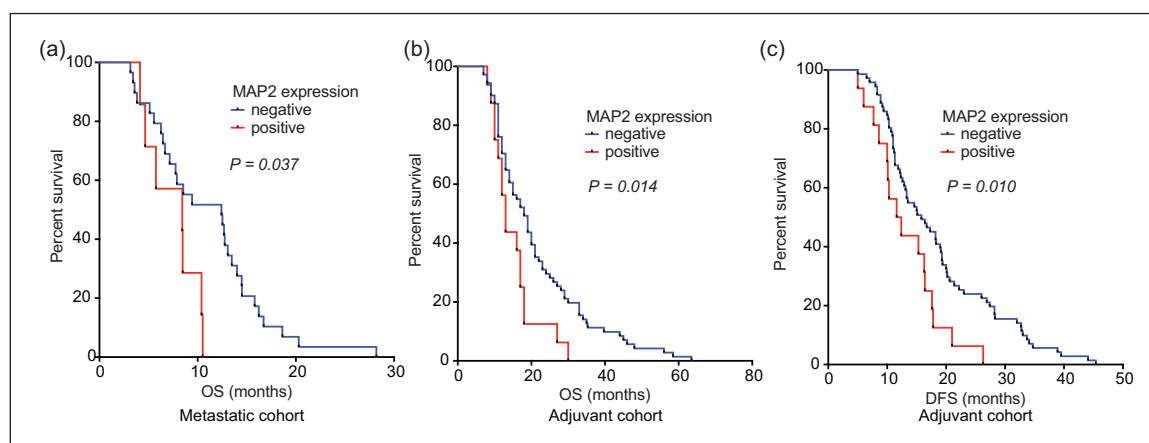


**Figure 4.** Correlation of MAP2 expression and OS and DFS upon gemcitabine treatment. (a) The Kaplan–Meier curves showed a correlation of MAP2 expression and OS in the palliative setting. In this first cohort 7 patients out of 36 had a positive MAP2 expression. (b) In the second cohort 16 out of 86 patients had a positive MAP2 staining of their primary tumour. (c) This expression correlates with poorer OS and DFS after gemcitabine adjuvant therapy. DFS, disease-free survival; MAP2, microtubule-associated protein 2; OS, overall survival.

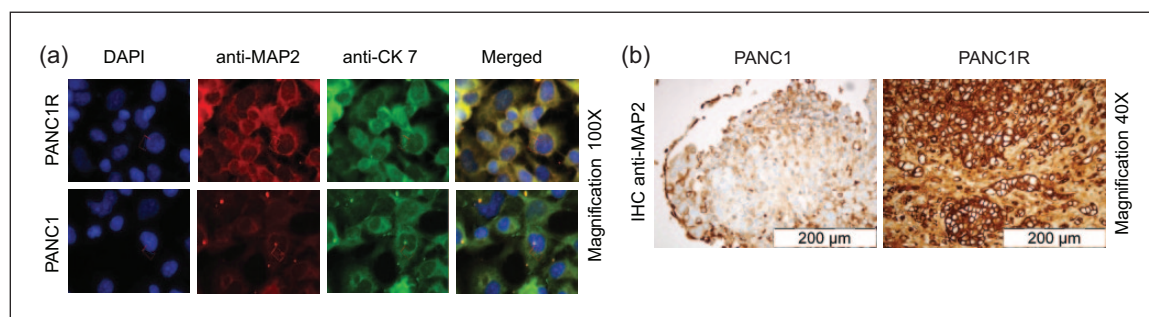


**Figure 5.** Immunofluorescence and immunohistochemistry of MAP2 in PANC1 and PANC1R cells and xenografts. (a) Immunofluorescence of PANC1 and PANC1R cells grown in chamber slides, and imaged at 100 $\times$  magnification, showing a strong MAP2 (red) cytoplasmic staining in the PANC1R cells and low expression in PANC1, confirming our proteomic analysis. CK7 staining was performed as positive control (green), and DAPI was used to stain the nuclei (blue). This phenotype was conserved in our xenograft model as is shown by IHC (b), where MAP2 expression was overexpressed in the PANC1R tumours *in vivo*. DAPI, 4',6-diamidino-2-phenylindole; DFS, disease-free survival; IHC, immunohistochemistry; MAP2, microtubule-associated protein 2; OS, overall survival; PANC1, gemcitabine-sensitive cell line; PANC1R, gemcitabine-resistant PANC1 cell line.

the palliative or adjuvant setting. In both cohorts, expression of MAP2 was correlated with poorer survival and thus, reduced treatment response.

The protein MAP2 has an important microtubule stabilization function<sup>30</sup> and is required for neurite outgrowth.<sup>31</sup> It has been described as a marker of neuronal differentiation and interacts with tubulins. Phosphorylation of MAP2 is an important regulator of its function, thus guiding microtubule dynamics.<sup>32–34</sup> Importantly, microtubules have an important function in intracellular transport machinery.<sup>35</sup> Changing microtubule dynamics by higher expression of MAP2 might result in

changed drug transport and efficacy intracellularly. Cytotoxic agents that act as microtubule polymerization stabilizers, like docetaxel, paclitaxel and its albumin-bound derivative nab-paclitaxel, function *via* multiple pathways that involve MAP2. These anticancer drugs inhibit the disassembly of polymerized microtubules. Subsequently, this aberrant stabilization results in mitotic cell cycle arrest or multispindle segregation, and cell death.<sup>36</sup> Interestingly, paclitaxel was shown to increase assembly of MAP2 onto polymerizing tubulins.<sup>37</sup> High MAP2 expression in mouse PDAC cell lines was correlated with sensitivity for docetaxel.<sup>38</sup> We did not observe an

increased sensitivity for docetaxel but identified an increased sensitivity for paclitaxel. The association between paclitaxel and MAP2 assembly on tubulins could explain our observation of increased sensitivity of gemcitabine-resistant cells to paclitaxel treatment and increased stable microtubules upon treatment with paclitaxel.

A previous study showed that modulation of microtubule dynamics by the silencing of tubulin binding cofactor C and cell cycle distribution enhanced the sensitivity to gemcitabine in breast cancer cells.<sup>39</sup> Furthermore, the combination of the benzophenone analogue S516, which changed the cellular microtubule network, with gemcitabine significantly delayed the growth of lung cancer tumours as compared with control and gemcitabine alone.<sup>40</sup>

Similarly, we identified an increased cytotoxic effect of combination treatment with gemcitabine in resistant cells, which provides a functional rationale for gemcitabine/nab-paclitaxel regimens in the metastatic and possibly the (neo)adjuvant setting. Our results suggest that gemcitabine-resistant cells are targeted effectively by (nab-) paclitaxel *in vitro* and *in vivo*, explaining the effectiveness of this combination therapy in the clinic.<sup>41</sup>

Expression of MAP2 has previously been described in several other solid tumours, such as oral squamous carcinoma,<sup>42</sup> lung cancer<sup>43</sup> and breast cancer.<sup>44</sup> Importantly, in two studies evaluating clinical samples from patients with breast cancer treated with taxanes, MAP2 was identified as a predictive marker for clinical response<sup>44,45</sup> in line with our results of sensitivity to (nab)-paclitaxel. Lack of expression of MAP2 was associated with significantly longer DFS and OS upon monotherapy with gemcitabine in our two cohorts, evoking the question of its potential as prognostic or predictive marker for gemcitabine response. Expression of MAP2 showed an association with gemcitabine sensitivity in cell lines as well. This biomarker can be essential to select patients in advance for taxane-based combination regimens. Further prospective trials to establish its predictive value in the adjuvant setting after a nab-paclitaxel/gemcitabine combination are therefore warranted.

Another interesting result of the present study is that the gemcitabine-resistant cells were capable of establishing xenograft tumours significantly

better than their parental cells. This indicates a higher clonogenic potential, a CSC characteristic previously associated with gemcitabine resistance.<sup>13</sup> In our proteomic screen, NES was identified as significantly upregulated. NES has previously been described as a CSC marker in pancreatic cancer,<sup>46,47</sup> as well as in cells which are known to feature chemoresistance.<sup>12</sup> However, although identified in our proteomic analysis, we did not detect this protein in TMAs with the current antibody. A possible reason might be low expression of this marker; however, this hampers the potential for clinical implementation. Another potential predictive marker identified from the proteomic screen, ANK3, has not been extensively described in cancer. It plays an important role in axon initiation and functions as an anchorage between membrane and cytoskeleton.<sup>48</sup> Even though we validated this protein as upregulated in our cell-line model, it was not a prognostic marker in our gemcitabine treated cohort. Of note, ANK3 has different isoforms and our western blot analysis showed multiple bands. Unfortunately, multiple bands are well-known issues of antibody-based validation. This might also explain why we could not validate the predictive results of ANK3 in our clinical data. These results also highlight the limitations of this study, namely the caution that is desired with a discovery analysis on a cell-line model instead of patient material. However, by implementation of clinical validation cohorts treated by gemcitabine monotherapy, an additional confirmation has been performed to conclude our clinically relevant findings.

The lethality of PDAC remains a problem to be solved in the upcoming decades. Our findings support the current trend towards combination therapy for the treatment of patients suffering from pancreatic cancer. Chemotherapeutic regimens for PDAC have recently shifted towards combination of multiple cytotoxic agents. Landmark trials have indeed demonstrated significant improvements in survival when gemcitabine was supplemented with nab-paclitaxel<sup>28</sup> or substituted for the more aggressive FOLFIRINOX (folic acid, fluorouracil, irinotecan, oxaliplatin) combination.<sup>2</sup> A shift towards combination treatment in the adjuvant setting is currently tested in clinical trials. Addition of capecitabine to the backbone of adjuvant gemcitabine was shown to increase the survival benefit by an additional 3 months.<sup>49</sup> Also, the Unicancer GI PRODIGE 24/CCTG PA.6 study recently showed an increase in OS of almost 20 months for adjuvant

treatment with FOLFIRINOX.<sup>50</sup> Addition of nab-paclitaxel to gemcitabine after resection is currently being evaluated (ClinicalTrials.gov identifier: NCT02023021). Part of the success of combination therapy might be, as our results imply, due to cytotoxic effect of resistant cells by additional chemotherapeutics. Although promising results of FOLFIRINOX in attacking PDAC, gemcitabine-based therapy remains commonly advised as second-line therapy and for patients with reduced physical reserve.<sup>51</sup> Thus, gemcitabine resistance still needs to be addressed in the upcoming years.

The present study has several limitations. Firstly, our most promising marker MAP2 was identified in only a cell-line resistance model. Additional models and knock-out experiments would be of interest to evaluate and validate the role of MAP2 in gemcitabine resistance in depth. To overcome the scarcity of gemcitabine-resistance models, we validated our result in two PDAC patient cohorts and a panel of cell lines. Additionally, we had a relatively low yield of xenograft tumours from the original PANC1 cells. This might be caused by the use of a nude mice strain, which retains a native immune response. However, the exceptional take rate of our gemcitabine-resistant cells is thereby emphasized. Finally, since multiple new drug regimens are under development for the treatment of PDAC, correlation as a predictive marker for other cytostatic agents would enhance the importance of our findings.

### Conclusion

By the use of powerful high-throughput proteomic techniques, we unravelled new differentially expressed proteins in a gemcitabine-resistant model of PDAC, including MAP2. Expression of this protein was correlated with a worse clinical outcome in patients with PDAC treated with gemcitabine. Further, we obtained preclinical data, *in vitro* and *in vivo*, showing that (nab-)/paclitaxel was effective against resistant/MAP2-overexpression cells, supporting new studies on this biomarker both to predict gemcitabine resistance and to guide better therapeutic choices.

### Acknowledgements

We would like to acknowledge Steve Sastra and Carmine Palermo for their assistance with mouse experiments and the patients for participating in the study. Further, we would like to acknowledge Dr M. Bugiani from the Department of Pathology

(VU University Medical Center) for the FFPE material from the tissues of the brain cortex.

Connie R. Jimenez, Maarten F. Bijlsma and Elisa Giovannetti contributed equally to this work.

TLL performed proteomic analysis, experimental work and wrote the manuscript. BEH and GK assisted with experimental work. NF performed immunohistochemistry and clinical data analysis. SRP and TVP were responsible for experimental design, MS/MS and bioinformatic analysis. KPOO, GK and HWML designed experiments and reviewed the manuscript. CRJ, MFB, EG were responsible for experimental design and helped to write the manuscript.

### Funding

This work was supported by the Cancer Center Amsterdam (Alliantie-AIO grant September 2014, the Netherlands), the Bennink Foundation (the Netherlands), Italian Association for Cancer Research (AIRC/Start-Up, Italy), Lisa Waller Hayes Foundation (the Netherlands), KWF Dutch Cancer Society (KWF project 10212 and 10401, the Netherlands) and NIH (1R01CA215607 and 1R21CA188857).

### Conflict of interest statement

MFB has received research funding from Celgene for a different study. This party was not involved in designing the study or drafting the manuscript.

### Ethics approval and consent to participate

The animal study has been approved by the Institutional Animal Care and Use Committee of the Columbia University (IACUC number AC-AAAQ1415). The study of clinical cohorts has been approved by the local medical ethical committee of Pisa University (Medical Ethical number 3909). The study was performed in accordance with the Declaration of Helsinki.

### Availability of data and material

Raw proteomics data has been deposited on ProteomeXchange under accession PXD010112.

### Supplemental material

Supplemental material for this article is available online.

### ORCID iDs

Tessa Ya Sung Le Large  <https://orcid.org/0000-0002-4273-7217>

Thang V. Pham  <https://orcid.org/0000-0003-0333-2492>

## References


1. Grasso C, Jansen G and Giovannetti E. Drug resistance in pancreatic cancer: Impact of altered energy metabolism. *Crit Rev Oncol Hematol*. 2017; 114: 139–152.
2. Conroy T, Desseigne F, Ychou M, *et al.* FOLFIRINOX versus gemcitabine for metastatic pancreatic cancer. *N Engl J Med* 2011; 364: 1817–1825.
3. Oettle H, Neuhaus P, Hochhaus A, *et al.* Adjuvant chemotherapy with gemcitabine and long-term outcomes among patients with resected pancreatic cancer: the CONKO-001 randomized trial. *JAMA* 2013; 310: 1473–1481.
4. Stocken DD, Ghaneh P, Cunningham D, *et al.* Adjuvant chemotherapy with fluorouracil plus folinic acid vs gemcitabine following pancreatic cancer resection: a randomized controlled trial. *JAMA* 2011; 304: 1073–1081.
5. Le N, Vinci A, Schober M, *et al.* Real-world clinical practice of intensified chemotherapies for metastatic pancreatic cancer: results from a pan-European questionnaire study. *Digestion* 2017; 94: 222–229.
6. Alvarellos ML, Lamba J, Sangkuhl K, *et al.* PharmGKB summary: gemcitabine pathway. *Pharmacogenet Genomics* 2014; 24: 564–574.
7. Labori KJ, Katz MH, Tzeng CW, *et al.* Impact of early disease progression and surgical complications on adjuvant chemotherapy completion rates and survival in patients undergoing the surgery first approach for resectable pancreatic ductal adenocarcinoma - A population-based cohort study. *Acta Oncol (Madr)* 2016; 55: 265–277.
8. Wehr AY, Furth EE, Sangar V, *et al.* Analysis of the human pancreatic stellate cell secreted proteome. *Pancreas* 2011; 40: 557–566.
9. Sherman MH, Yu RT, Engle DD, *et al.* Vitamin D receptor-mediated stromal reprogramming suppresses pancreatitis and enhances pancreatic cancer therapy. *Cell* 2014; 159: 80–93.
10. Hessmann E, Patzak MS, Klein L, *et al.* Fibroblast drug scavenging increases intratumoural gemcitabine accumulation in murine pancreas cancer. *Gut* 2017; 67: 497–507.
11. Ireland L, Santos A, Ahmed MS, *et al.* Chemoresistance in pancreatic cancer is driven by stroma-derived insulin-like growth factors. *Cancer Res* 2016; 76: 6851–6863.
12. Van den Broeck A, Gremeaux L, Topal B, *et al.* Human pancreatic adenocarcinoma contains a side population resistant to gemcitabine. *BMC Cancer* 2012; 12: 354.
13. Quint K, Tonigold M, Di Fazio P, *et al.* Pancreatic cancer cells surviving gemcitabine treatment express markers of stem cell differentiation and epithelial-mesenchymal transition. *Int J Oncol* 2012; 41: 2093–2102.
14. Zheng X, Carstens JL, Kim J, *et al.* Epithelial-to-mesenchymal transition is dispensable for metastasis but induces chemoresistance in pancreatic cancer. *Nature* 2015; 527: 525–530.
15. Avan A, Caretti V, Funel N, *et al.* Crizotinib inhibits metabolic inactivation of gemcitabine in c-Met-driven pancreatic carcinoma. *Cancer Res* 2013; 73: 6745–6756.
16. Piersma SR, Knol JC, de Reus I, *et al.* Feasibility of label-free phosphoproteomics and application to base-line signaling of colorectal cancer cell lines. *J Proteomics* 2015; 127: 247–258.
17. Piersma SR, Warmoes MO, de Wit M, *et al.* Whole gel processing procedure for GeLC-MS/MS based proteomics. *Proteome Sci* 2013; 11: 17.
18. Cox J and Mann M. MaxQuant enables high peptide identification rates individualized p.p.b.-range mass accuracies and proteome-wide protein quantification. *Nat Biotechnol* 2008; 26: 1367–1372.
19. Vizcaino JA, Csordas A, Del-Toro N, *et al.* 2016 update of the PRIDE database and its related tools. *Nucleic Acids Res* 2016; 44: D447–D456.
20. Giovannetti E, Wang Q, Avan A, *et al.* Role of CYB5A in pancreatic cancer prognosis and autophagy modulation. *J Natl Cancer Inst* 2014; 106: djt346.
21. Leon L, Gemelli M, Sciarrillo R, *et al.* Synergistic activity of the c-Met and tubulin inhibitor tivantinib (ARQ197) with pemetrexed in mesothelioma cells. *Curr Drug Targets* 2014; 15: 1331–1340.
22. Pham TV, Piersma SR, Warmoes M, *et al.* On the beta-binomial model for analysis of spectral count data in label-free tandem mass spectrometry-based proteomics. *Bioinformatics* 2009; 26: 363–369.
23. Bindea G, Mlecnik B, Hackl H, *et al.* ClueGO: a Cytoscape plug-in to decipher functionally grouped gene ontology and pathway annotation networks. *Bioinformatics* 2009; 25: 1091–1093.
24. Harsha HC and Pandey A. Phosphoproteomics in cancer. *Mol Oncol* 2010; 4: 482–495.
25. Sharma A. Chemoresistance in cancer cells: exosomes as potential regulators of therapeutic tumor heterogeneity. *Nanomedicine* 2017; 12: 2137–2148.

26. Toffalorio F, Santarpia M, Radice D, *et al.* 5'-nucleotidase cN-II emerges as a new predictive biomarker of response to gemcitabine/platinum combination chemotherapy in non-small cell lung cancer. *Oncotarget* 2018; 9: 16437–16450.
27. Wang J, Yeung BZ, Cui M, *et al.* Exosome is a mechanism of intercellular drug transfer: application of quantitative pharmacology. *J Control Release* 2017; 268: 147–158.
28. Von Hoff DD, Ervin T, Arena FP, *et al.* Increased survival in pancreatic cancer with nab-paclitaxel plus gemcitabine. *N Engl J Med* 2013; 369: 1691–1703.
29. Sciarillo R, Wojtuszkiewicz A, Kooi IE, *et al.* Using RNA-sequencing to detect novel splice variants related to drug resistance in in vitro cancer models. *J Vis Exp* 2016. doi: 10.3791/54714
30. Sánchez C, Díaz-Nido J and Avila J. Phosphorylation of microtubule-associated protein 2 (MAP2) and its relevance for the regulation of the neuronal cytoskeleton function. *Prog Neurobiol* 2000; 61: 133–168.
31. Sharma N, Kress Y and Shafit-Zagardo B. Antisense MAP-2 oligonucleotides induce changes in microtubule assembly and neuritic elongation in pre-existing neurites of rat cortical neurons. *Cell Motil Cytoskeleton* 1994; 27: 234–247.
32. Ka mierzak-Bara ska J, P czek Ł, Przygodzka P, *et al.* Downregulation of striatin leads to hyperphosphorylation of MAP2, induces depolymerization of microtubules and inhibits proliferation of HEK293T cells. *FEBS Lett* 2015; 589: 222–230.
33. Akhmanova A and Steinmetz MO. Control of microtubule organization and dynamics: two ends in the limelight. *Nat Rev Mol Cell Biol* 2015; 16: 711–726.
34. Ebnet A, Drewes G, Mandelkow E, *et al.* Phosphorylation of MAP2c and MAP4 by MARK kinases leads to the destabilization of microtubules in cells. *Cell Motil Cytoskeleton* 1999; 224: 209–224.
35. Barlan K and Gelfand VI. Microtubule-based transport and the distribution, tethering, and organization of organelles. *Cold Spring Harb Perspect Biol* 2017; 9: pii: a025817.
36. Weaver BA. How Taxol/paclitaxel kills cancer cells. *Mol Biol Cell* 2014; 25: 2677–2681.
37. Nishio K, Arioka H, Ishida T, *et al.* Enhanced interaction between tubulin and microtubule-associated protein 2 via inhibition of MAP kinase and CDC2 kinase by paclitaxel. *Int J Cancer* 1995; 63: 688–693.
38. Veitia R, David S, Barbier P, *et al.* Proteolysis of microtubule associated protein 2 and sensitivity of pancreatic tumours to docetaxel. *Br J Cancer* 2000; 83: 544–549.
39. Hage-Sleiman R, Herveau S, Matera EL, *et al.* Silencing of tubulin binding cofactor C modifies microtubule dynamics and cell cycle distribution and enhances sensitivity to gemcitabine in breast cancer cells. *Mol Cancer Ther* 2011; 10: 303–312.
40. Moon CH, Lee SJ, Lee HY, *et al.* CKD-516 displays vascular disrupting properties and enhances anti-tumor activity in combination with chemotherapy in a murine tumor model. *Invest New Drugs* 2014; 32: 400–411.
41. Goldstein D, El-Maraghi RH, Hammel P, *et al.* Nab-paclitaxel plus gemcitabine for metastatic pancreatic cancer: Long-term survival from a phase III trial. *J Natl Cancer Inst* 2015; 107: 1–10.
42. Liu SY, Chen YT, Tseng MY, *et al.* Involvement of microtubule-associated protein 2 (MAP2) in oral cancer cell motility: a novel biological function of MAP2 in non-neuronal cells. *Biochem Biophys Res Commun* 2008; 366: 520–525.
43. Tanaka K and Terasaki T. Immunocytochemical expression of microtubule-associated protein-2 (MAP-2) in small cell lung cancer cell lines with neuronal-like processes. *Japanese J Cancer Res* 2002; 93: 699–705.
44. Bauer JA, Chakravarthy AB, Rosenbluth JM, *et al.* Identification of markers of taxane sensitivity using proteomic and genomic analyses of breast tumors from patients receiving neoadjuvant paclitaxel and radiation. *Clin Cancer Res* 2010; 16: 681–690.
45. Kolacinska A, Fendler W, Szemraj J, *et al.* Gene expression and pathologic response to neoadjuvant chemotherapy in breast cancer. *Mol Biol Rep* 2012; 39: 7435–7441.
46. Yamahatsu K, Matsuda Y, Ishiwata T, *et al.* Nestin as a novel therapeutic target for pancreatic cancer via tumor angiogenesis. *Int J Oncol* 2012; 40: 1345–1357.
47. Matsuda Y, Yoshimura H, Ueda J, *et al.* Nestin delineates pancreatic cancer stem cells in metastatic foci of NOD/Shi-scid IL2Rγ(null) (NOG) mice. *Am J Pathol* 2014; 184: 674–685.
48. Leterrier C, Clerc N, Rueda-Boroni F, Montersino A, Dargent B and Castets F. Ankyrin G membrane partners drive the establishment and maintenance of the axon initial segment. *Front Cell Neurosci* 2017; 11: 1–14.



49. Neoptolemos JP, Palmer DH, Ghaneh P, *et al.* Comparison of adjuvant gemcitabine and capecitabine with gemcitabine monotherapy in patients with resected pancreatic cancer (ESPAC-4): a multicentre, open-label, randomised, phase 3 trial. *Lancet* 2017; 389: 1011–1024.
50. Monday P, Conroy T, Hammel P, *et al.* Unicancer GI PRODIGE 24/CCTG PA.6 trial: a multicenter international randomized phase III trial of adjuvant mFOLFIRINOX versus gemcitabine (gem) in patients with resected pancreatic ductal adenocarcinomas. *J Clin Oncol* 2018; 36(Suppl. 18): LBA4001.
51. Sohal DPS, Kennedy EB, Khorana A, *et al.* Metastatic pancreatic cancer: ASCO clinical practice guideline update. *J Clin Oncol* 2018; 36: 2545–2556.

Visit SAGE journals online  
[journals.sagepub.com/  
home/tam](http://journals.sagepub.com/home/tam)

 SAGE journals